PAPER

Check for updates

Characterization of regulatory T cell expansion for manufacturing cellular immunotherapies†

David A. McBride, [ID] [a,b,c] Matthew D. Kerr, [a,b,c] Shinya L. Wai, [a] Yvonne Y. Yee, [a,b] Dora A. Ogbonna [a,b] and Nisarg J. Shah [ID] *[a,b,c,d,e]

Regulatory T cells (T$_{regs}$) are critical mediators of peripheral immune tolerance. T$_{regs}$ suppress immune activation against self-antigens and are the focus of cell-based therapies for autoimmune diseases. However, T$_{regs}$ circulate at a very low frequency in blood, limiting the number of cells that can be isolated by leukapheresis. To effectively expand T$_{regs}$ *ex vivo* for cell therapy, we report the metabolic modulation of T cells using mono-(6-amino-6-deoxy)-β-cyclodextrin (βCD-NH$_2$) encapsulated rapamycin (Rapa). Encapsulating Rapa in β-cyclodextrin increased its aqueous solubility ~154-fold and maintained bioactivity for at least 30 days. βCD-NH$_2$-Rapa complexes (CRCs) enriched the fraction of CD4$^+$CD25$^+$FoxP3$^+$ mouse T (mT) cells and human T (hT) cells up to 6-fold and up to 2-fold respectively and suppressed the overall expansion of effector T cells by 5-fold in both species. Combining CRCs and transforming growth factor beta-1 (TGF-β1) synergistically promoted the expansion of CD4$^+$CD25$^+$FoxP3$^+$ T cells. CRCs significantly reduced the fraction of pro-inflammatory interferon-gamma (IFN-γ) expressing CD4$^+$ T cells, suppressing this Th1-associated cytokine while enhancing the fraction of IFN-γ$^-$ tumor necrosis factor-alpha (TNF-α) expressing CD4$^+$ T cells. We developed a model using kinetic rate equations to describe the influence of the initial fraction of naïve T cells on the enrichment of T$_{regs}$ *in vitro*. The model related the differences in the expansion kinetics of mT and hT cells to their susceptibility for immunophenotypic modulation. CRCs may be an effective and potent means for phenotypic modulation of T cells and the enrichment of T$_{regs}$ *in vitro*. Our findings contribute to the development of experimental and analytical techniques for manufacturing T$_{reg}$ based immunotherapies.

Introduction

Regulatory T cells (T$_{regs}$) are T cell subset that suppress aberrant activation of self-reactive effector lymphocytes and are widely regarded as the primary mediators of peripheral tolerance.[1] Cell-based therapy using T$_{regs}$ effectively treats autoimmune diseases such as arthritis and type 1 diabetes in animal models and at least one clinical trial (NCT02772679) is underway to evaluate efficacy in humans.[2–5] However, sourcing T$_{regs}$ from leukapheresis is inefficient as they circulate at a low

frequency (3–5%) in the blood and therefore *ex vivo* expansion is required to enhance their numbers. Current expansion methods, which use natural or artificial antigen-presenting cells and interleukin-2 (IL-2), induce the activation of not only T$_{regs}$ but also conventional T cells.[6,7] Because T$_{regs}$ divide more slowly than effector T cells, the latter may significantly outgrow T$_{regs}$.[8] Therefore, T$_{regs}$ must be highly purified and sorted to avoid transfusion of T effector cells, which can be challenging.[9] Furthermore, T$_{reg}$-mediated suppression could diminish after repetitive stimulation.[10] These requirements for expanding and isolating T$_{regs}$ *ex vivo* limit their use for cell therapy.

One method to efficiently enhance T$_{regs}$ is by expanding T cells in medium containing rapamycin (Rapa), a carboxylic lactone–lactam triene macrolide with antifungal, antitumor and anti-inflammatory properties.[11] Rapa is administered orally or intravenously for systemic immunosuppression to prevent organ transplant rejection.[12,13] Rapa inhibits the serine/threonine protein kinase called mammalian target of rapamycin (mTOR), which is involved in a broad range of physiological processes linked to the control of cell cycle.[14] Consistent with this mechanism, Rapa locks T cell-cycle pro-

[a]*Department of Nanoengineering, University of California, San Diego, La Jolla, CA 92093, USA. E-mail: nshah@ucsd.edu*
[b]*Chemical Engineering Program, University of California, San Diego, La Jolla, CA 92093, USA*
[c]*Center for Nano-Immuno Engineering, University of California, San Diego, La Jolla, CA 92093, USA*
[d]*Program in Immunology, University of California, San Diego, La Jolla, CA 92093, USA*
[e]*San Diego Center for Precision Immunotherapy, Moores Cancer Center, University of California, San Diego, La Jolla, CA 92093, USA*
†Electronic supplementary information (ESI) available. See DOI: 10.1039/d0bm00622j

gression from G_1 to S phase after activation, enhances T_{reg} number and maintains their function by preferentially reducing proliferation of effector T cells, while minimally affecting the regulatory T cell subset.[15–18] Rapa induces operational tolerance and suppresses the proliferation of effector T cells and decreases the production of proinflammatory cytokines by T cells *in vivo* and *in vitro*.[19–22] However, the poor aqueous solubility of Rapa, low stability in serum and short half-life (~10 hours at 37 °C) limits bioavailability and uptake by T cells.[23,24]

Cyclodextrin monomers are well characterized cyclic oligosaccharides that form complexes with drug molecules *via* secondary hydrophobic interactions.[25] The formation of inclusion complexes with small molecule drugs delays the rate of drug release beyond that of diffusion alone.[26] The most common pharmaceutical applications of beta-cyclodextrin (βCD) derivatives are as excipients in clinical drug formulations to enhance the aqueous solubility of the complexed species, to improve the aqueous stability, photostability, and bioavailability of complexed drugs.[27] *In vivo*, βCDs have been shown to enhance drug absorption and oral bioavailability as well as facilitate drug transport across physiologic barriers and biological membranes. Complexes of Rapa with βCD derivatives improve solubility and stability of Rapa, while preserving bioactivity.[28,29] Prior experiments have quantified a K_d between Rapa and βCD derivatives in the micromolar range.[30] The high supramolecular affinity prolongs its bioavailability and therefore is an attractive choice for formulations to promote enhancements of the half-life of Rapa *in vitro*. The extended half-life of Rapa could synergize with other potent inducers of regulatory T cells, including transforming growth factor-beta (TGF-β1), which mediates the transition of naïve T cells toward a regulatory phenotype with potent immunosuppressive potential.[31]

To promote the enrichment of T_{regs} *in vitro*, we encapsulated and characterized the function of Rapa encapsulated in mono-(6-amino-6-deoxy)-β-cyclodextrin (βCD-NH$_2$) forming cyclodextrin-Rapa complexes (CRCs). CRCs enhanced the solubility of Rapa in water 154-fold and maintained bioactivity of Rapa for at least 30 days in solution. CRCs enriched the fraction by 5-fold of T_{regs} *in vitro* from both PBMC-isolated human T (hT) cells and splenocyte-isolated mouse T (mT) cells. CRCs synergize with TGF-β1 to enhance the enrichment of murine T_{regs}. The combination also enhanced the fraction of human T_{regs} over single factor treatments. CRCs reduced interferon-gamma (IFN-γ) expression by T cells and increased the fraction of T cells that expressed tumor necrosis factor-α (TNF-α) without IFN-γ. In hT cells, combining CRC and TGF-β1 further enhanced the enrichment of IFN-γ⁻ TNF-α⁺ T cells, while in mT cells the addition of TGF-β1 increased the fraction of IFN-γ⁺ T cells, both alone and in combination with CRCs.

We developed a computational model to describe the expansion kinetics of T_{reg} enrichment. The model recapitulated key features associated with CRCs and TGF-β1 individually and in combination on T_{reg} expansion. A sensitivity analysis demonstrated that the initial fraction of naïve T cells is critical for ensuring a high fraction of T_{regs}. CRCs are a potent delivery system for Rapa to enhance the preferential expansion of T_{regs} and inhibiting inflammatory T cells, and the model may serve to guide T_{reg} expansion for manufacturing cellular immunotherapies.

Materials and methods

Materials

Basal T cell culture media was prepared from RPMI medium 1640 powder (Gibco) supplemented with 10% HI-FBS, 1% penicillin–streptomycin, 1 mM sodium pyruvate, 50 μM β-mercaptoethanol and 0.1 mM non-essential amino acids. Primary mT and hT cell media used for expansion was further supplemented with 50 IU mL^{-1} murine recombinant IL-2 (Peprotech) and 50 IU mL^{-1} human recombinant IL-2 (Biolegend), respectively. Rapa was purchased from LC Laboratories. Mono-(6-amino-6-deoxy)-β-cyclodextrin, with an upper solubility limit of 4.2 wt% in water, was purchased from Cavcon (CAS#: 29390-67-8). Dimethylsulfoxide (DMSO) was purchased from Sigma-Aldrich.

Generation and characterization of CRCs

CRCs were prepared by first creating 0%, 1%, 2%, 3%, and 4% (wt/v) solutions of βCD-NH$_2$ in DI water. 500 μL of each solution was added to 1 mg of Rapa and vortexed at 3200 rpm for 5 minutes, and then agitation was maintained at 1500 rpm until sampling. The inclusion complexes were equilibrated over 7 days as previously reported. Subsequently, the solution was spun down (21 000 rcf, 5 min) and the supernatant was collected and analyzed on day 7. The amount of Rapa in the supernatant was analyzed using UV-vis spectrophotometry (λ = 278 nm) (Fig. S1a†).

Primary T cell isolation

All animal procedures were approved by the Institutional Animal Care and Use Committee at UC San Diego. Primary murine T cells were freshly isolated from C57BL/6J mice. A single cell suspension of splenocytes was created and T cells were isolated *via* magnetic depletion using CD4$^+$ or pan-T cell isolation kits (Miltenyi Biotec) according to the manufacturer's recommendations. Murine T cells were not cryopreserved as the cells were found to be sensitive to DMSO at concentrations greater than 1%(v/v) and reconstituted murine T cells expanded less than freshly isolated cells (data not shown).

Primary hT cells were isolated from anonymous donor blood concentrate enriched in the buffy coat (Stanford Blood Bank and San Diego Blood Bank). PBMCs were enriched from buffy coat within 24 hours of collection using density separation in a Ficoll gradient (Lymphopure). PBMCs were then transferred to serum-free cell freezing media (Bambanker) and frozen overnight at −80 °C. Aliquots were then stored in liquid nitrogen and used within 6 months. Pan T cells were isolated from thawed PBMC aliquots using magnetic depletion (Dynabeads Untouched Human T cells, Invitrogen) according to the manufacturer's recommendations.

In vitro T cell expansion assays

Primary mT and hT cells were isolated as described above and resuspended in T cell culture media without IL-2. Mouse or human αCD3/αCD28 activator Dynabeads (Invitrogen) were added to mT and hT cells, respectively, according to manufacturer recommendations and cells were plated in 96 well plates. After one day of culture, recombinant murine or human IL-2 was added to cultures at a concentration of 50 IU mL^{-1} along with any factors being tested. On the seventh day of culture, cells were enumerated with cell counting using a hemocytometer and analyzed with flow cytometry. In cultures testing the suppressive effects of DMSO- or βCD-NH2-solubilized Rapa, Rapa was added at concentrations of 10, 100 or 1000 nM and TGF-β1 was used at 5 ng mL^{-1}. DMSO concentration was maintained across groups at a concentration of 0.1% (v/v). For CFSE analysis, cells were stained prior to activation with Dynabeads with CFSE (CFSE Cell Division Tracker Kit, Biolegend) according to manufacturer's instructions. Cells stained with CFSE were analyzed after 72 hours with flow cytometry.

Cytokine assay

Primary mT and hT cells were cultured as previously detailed. 5 days post activation with Dynabeads, the cells were restimulated with PMA and ionomycin and blocked with Brefeldin A (Cell Activation Kit with Brefeldin A, Biolegend) for 5 hours according to manufacturer's instructions. Cells were then washed, stained, and analyzed with flow cytometry.

Flow cytometry

Antibodies for anti-mouse CD25 (PC61), CD8α (53-6.7), CD4 (GK1.5), CD45 (30-F11), TNF-α (MP6-XT22), IFN-γ (XMG1.2), and anti-human CD8α (RPA-T8), CD4 (SK3), CD25 (M-A251), CD45 (HI30), TNF-α (Mab11), and IFN-γ (B27) were purchased from Biolegend. Antibodies for anti-mouse FoxP3 (FJK-16s) and anti-human FoxP3 (236A/E7), were purchased from eBioscience. Samples analyzed for FoxP3 expression were fixed and permeabilized using the FoxP3/Transcription Factor Staining Buffer Set (eBioscience) according to manufacturer supplies protocols. Samples analyzed for TNF-α and IFN-γ expression but not FoxP3 were fixed using the IC Fixation Buffer (eBioscience) and permeabilized using Permeabilization Buffer (eBioscience) according to manufacturer supplied protocols. All cells were gated based on forward and side scatter characteristics to limit debris. Gating for surface markers, cytokines, and FoxP3 were determined using fluorescence-minus-one controls.

Computational modeling and parameter analysis

To calculate the parameter values in the model we used data sets from our experiments. To determine the sensitivity of the model outputs to initial model regulatory T cell (T_r) fraction the model was initialized with 1%, 2%, and 3% T_r with a fixed model effector T cell (T_e) (36.5%) fraction and variable model naïve T cell (T_n) (62.5%, 61.5% and 60.5%). The range of initial

T_r values examined, as well as the starting T_e and T_n values, were informed by analysis of T cell isolations and naïve T cell staining for CD62L and CD44. To determine the sensitivity of the model to initial T_e fraction the model was initialized with 18.2%, 36.5% and 54.7% T_e, with a fixed T_r (2%) and variable T_n (79.8%, 61.5%, 43.3%). An Excel sheet detailing parameter calculation and all code used to generate the model may be found at https://github.com/Shah-Lab-UCSD/Treg_Enrichment_Model_In_Vitro. All code was written to be compatible with Python 3.7.6.

Results

Mono-(6-amino-6-deoxy)-beta-cyclodextrin increases aqueous solubility of Rapa

To test the encapsulation of Rapa and improve the aqueous solubility, we used the βCD mono-(6-amino-6-deoxy)-beta-cyclodextrin (βCD-NH$_2$), forming βCD-NH$_2$-Rapa inclusion complexes (Fig. 1a and b). We first measured loading of Rapa in 0–4% (w/v) βCD-NH$_2$s in deionized water (Fig. 1c). The loading of Rapa in the inclusion complexes was quantified using a standard curve (Fig. S1a†). The amount of Rapa in solution was proportional to the βCD-NH$_2$ concentration and achieved a maximum loading of 4.02 ± 0.52 mg mL^{-1} in a 4 wt% solution of βCD-NH$_2$ on day 7 (Fig. 1d). The supernatant of the solution prepared without βCD-NH$_2$ did not have a detectable amount of Rapa. To test the stability of the inclusion complex, CRC containing supernatant was transferred to new tubes that were incubated at room temperature over 30 days. In all samples, the amount of Rapa initially decreased and equilibrated after 7 days at 82.5% ± 1.7% of the initial concentration (Fig. 1e).

Rapa preferentially expands T$_{regs}$

To test the suppressive activity of Rapa on T cell proliferation and enriching regulatory T cells (T$_{regs}$), we measured its dose-dependent effect *in vitro*. mT cells were isolated from splenocytes using magnetic bead-based depletion. Approximately 90% of the cells were either CD4$^+$ or CD8$^+$ T cells post-enrichment (Fig. S1b†). We tested a broad range of Rapa concentrations (1 μM, 100 nM, 10 nM) (Fig. 2a) and measured fold-expansion and the frequency of CD4$^+$CD25$^+$FoxP3$^+$ T cells relative to the total number of CD4$^+$ T cells seven days post-activation. T cell expansion in 1 μM Rapa (5.26 ± 0.15) was comparable to 10 nM (6.13 ± 0.96) and 100 nM concentration (4.65 ± 0.63-fold expansion) (Fig. 2b), and were significantly lower compared to the Dynabead-only (25.8 ± 1.2) and DMSO controls (20.7 ± 1.2-fold expansion). The fraction of CD4$^+$ T cells that were also CD25$^+$FoxP3$^+$ was similar at 10 nM (10.3% ± 1.3%), 100 nM (10.3% ± 1.6%), and 1 μM (12.2% ± 0.7%) and significantly higher compared with the Dynabead-only (2.96% ± 1.51%) and DMSO controls (1.54% ± 0.78%) (Fig. 2c). To examine the effects of DMSO-solubilized Rapa on expansion of CD25^{hi} and CD25^{lo} CD4$^+$ T cell subsets, we conducted a proliferation assay using carboxyfluorescein succinimidyl ester
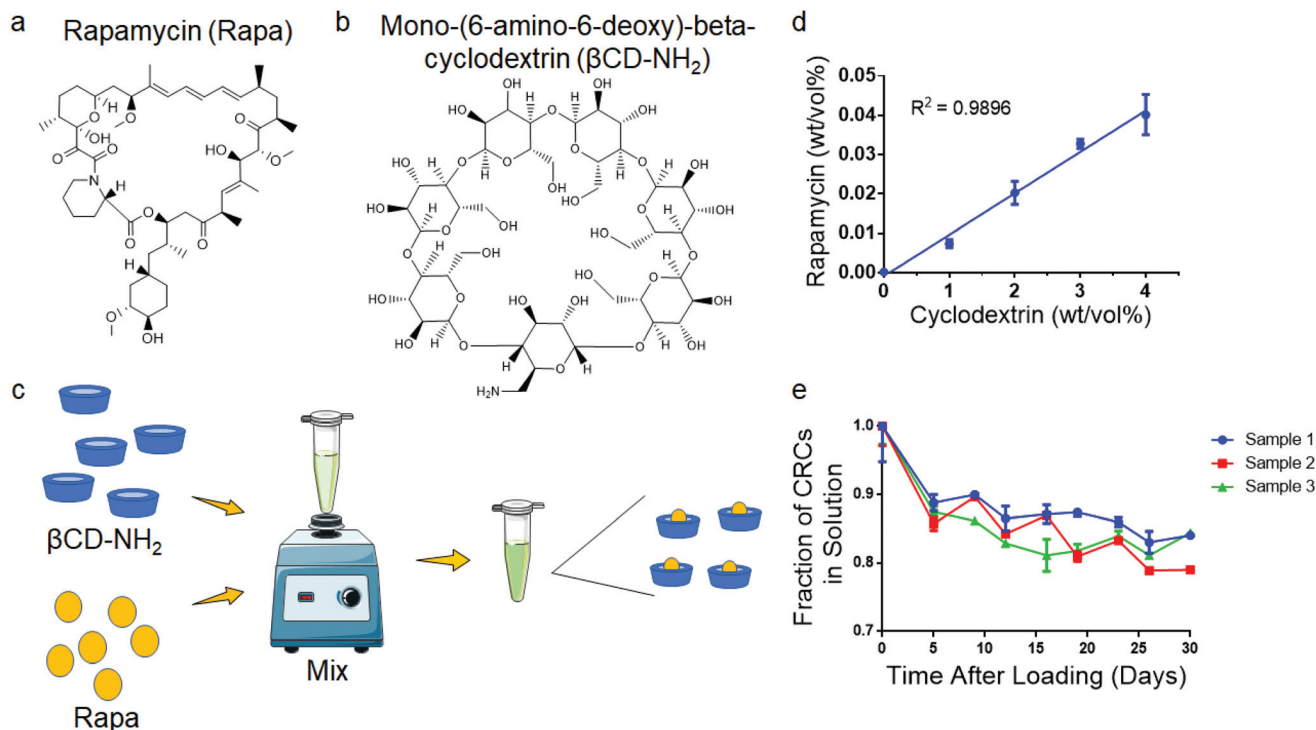
Fig. 1 Complexation with mono-(6-amino-6-deoxy)-beta-cyclodextrin enhances the aqueous solubility of rapamycin. Chemical structure of (a) rapamycin (Rapa) and (b) mono-(6-amino-deoxy)-beta-cyclodextrin (βCD-NH$_2$) (c) Schematic for βCD-Rapa complexes (CRC). (d) Quantification of the Rapa loading in βCD-NH$_2$. (e) Stability of CRC in solution over 30 days. Data in (d) represent the mean ± s.d. for n = 3 independent experiments. Data in e represent the mean mean ± s.d. for n = 3 technical replicates.

(CFSE). In the absence of Rapa, CD25^{lo} T cells proliferated more than CD25^{hi} T cells. When 100 nM Rapa was added, both CD25^{hi} and CD25^{lo} T cells proliferated a similar amount, with both groups expanding less than controls (Fig. S2a†).

Cyclodextrin-Rapa complexes potently suppress T cell proliferation

To test the bioactivity of Rapa encapsulated in CRCs, we compared the phenotypic modulation of murine T cells mediated by CRCs and Rapa solubilized in a DMSO carrier (Fig. 2d). In contrast to DMSO-solubilized Rapa, T cell expansion was strongly dependent on the concentration of CRCs, but unaffected by βCD-NH$_2$ alone (Fig. 2e). 10 nM CRCs did not substantially affect T cell expansion (21.4 ± 2.1-fold) compared to the Dynabead-only control (24.2 ± 1.2-fold). T cell expansion with 100 nM CRCs (14.4 ± 1.7-fold) and 1μM CRCs (6.93 ± 0.91-fold) was significantly lower than the Dynabead-only and βCD-NH$_2$ (24.1 ± 1.6-fold) controls. In addition, the suppression of T cell expansion mediated by 1μM CRCs was comparable to 100 nM DMSO-solubilized Rapa (7.81 ± 1.75-fold expansion). Similarly, the enrichment of CD4$^+$CD25$^+$FoxP3$^+$ murine T cells was comparable between the 10 nM CRC (1.46% ± 0.10%), Dynabead-only control (1.57% ± 0.25%), and βCD-NH$_2$ control (1.21% ± 0.21%) (Fig. 2f). These cells were significantly enriched with 100 nM CRC (2.29% ± 0.26%) and 1 μM CRC (5.86% ± 0.28%).

TGF-β1 and CRCs promote T$_{reg}$ enrichment through distinct mechanisms

To test if combinations of immunomodulatory factors might further enrich CD4$^+$CD25$^+$FoxP3$^+$ T$_{regs}$, we tested transforming growth factor-beta (TGF-β1) in combination with Rapa. Murine T cells were cultured in media containing either 5 ng mL^{-1} TGF-β1, 1 μM CRCs or both factors and quantified the expansion of T cells as well as the fraction of CD25$^+$FoxP3$^+$CD4$^+$ T cells (Fig. 3a). TGF-β1 alone did not suppress the expansion of T cells (26.8 ± 3.2-fold) relative to the Dynabead-only control (24.2 ± 1.2-fold). However, TGF-β1 in combination with 1 μM CRCs suppressed T cell expansion (6.73 ± 0.82-fold expansion) which was comparable to 1 μM CRCs alone (6.93 ± 0.91-fold expansion) (Fig. 3b). TGF-β1 in combination with 1 μM CRCs (21.1% ± 0.46%) increased the fraction of T$_{regs}$ more than TGF-β1 (10.8% ± 0.46%) or 1 μM CRCs (5.86% ± 0.28%) alone (Fig. 3c). Strikingly, this enrichment was greater than the sum of the enhancement mediated by either CRCs or TGF-β1 alone (Fig. 3d). We compared CD4$^+$FoxP3$^+$ T$_{reg}$ and the CD4$^+$FoxP3$^-$ T cell counts between the test groups (Fig. 3e). 100 nM and 1 μM CRCs reduced the number of total CD4$^+$FoxP3$^-$ cells compared with the Dynabead-only control but did not affect the number of T$_{reg}$. In contrast, TGF-β1 increased the number of T$_{reg}$ relative to control but did not significantly affect proliferation of CD4$^+$FoxP3$^-$ T cells. In combination, TGF-β1 and 1 μM CRC increased T$_{reg}$ and decreased CD4$^+$FoxP3$^-$ T cells.
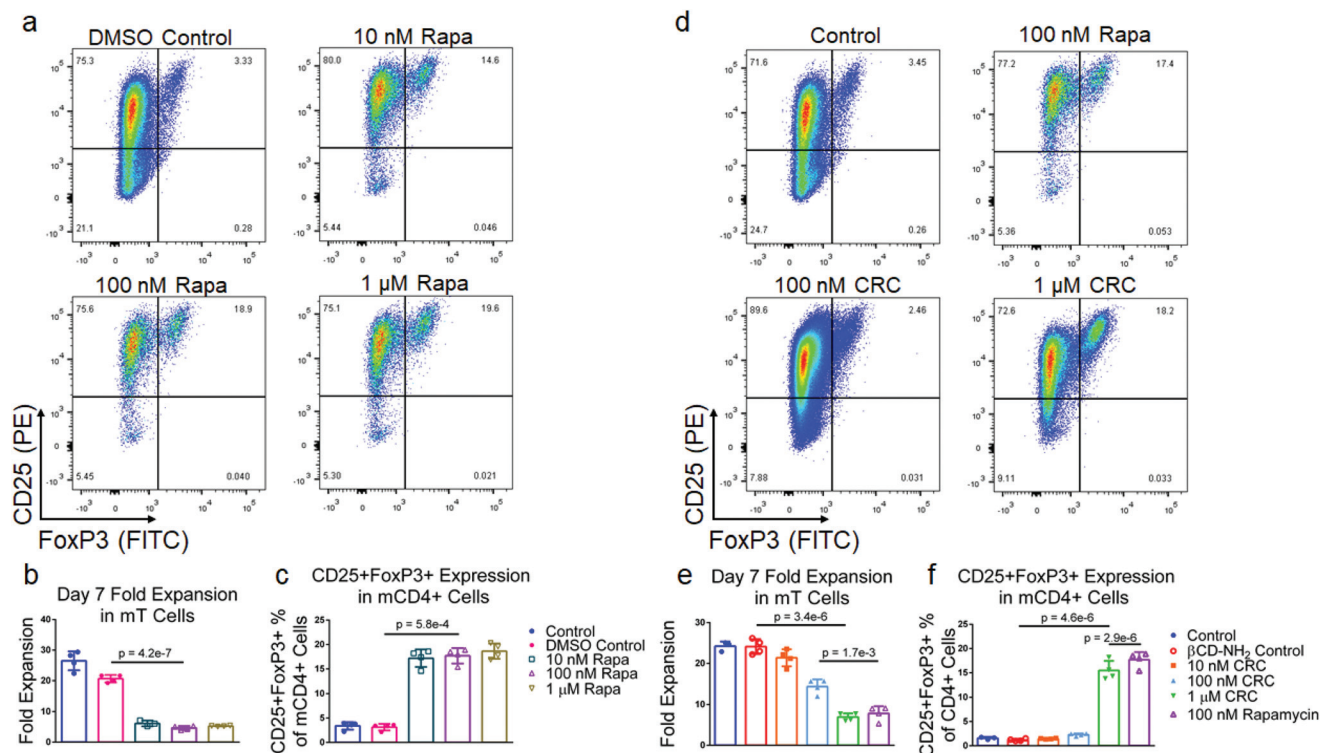
Fig. 2 Rapa and CRCs suppress mouse T cell expansion and enhance T_{regs}. (a) Representative flow cytometry plots of CD25$^+$FoxP3$^+$ CD4$^+$ mouse T (mT) cells. Quantification of the fold expansion of CD4$^+$ and CD8$^+$ T cells (b) and the fraction of CD4$^+$CD25$^+$FoxP3$^+$ T cells (c) after 7 days of expansion at a range of Rapa concentrations. (d) Representative flow cytometry plots of CD4$^+$CD25$^+$FoxP3$^+$ T cells. Quantification of the fold expansion of CD4$^+$ and CD8$^+$ T cells (e) and the fraction of CD25$^+$FoxP3$^+$ CD4$^+$ T cells (f) after 7 days of expansion at a range of CRC concentrations. Data represents the mean $\pm$ s.d. (n = 4). Experiments were repeated at least three times.

CRCs and TGF-β1 have opposing effects on IFNγ expression in murine T cells

As the immunophenotype of T cells is associated with its cytokine profile, we next measured the difference in production of pro-inflammatory cytokines in mT cells with combination of single factor CRCs and TGF-β1 (Fig. 4a and b). The fraction of CD4$^+$ IFN-γ$^+$ T cells was significantly depleted in CRC-treated cells (10.0% ± 0.6%) relative to Dynabead-only control (30.6% ± 2.9%). CD4$^+$ IFN-γ$^+$ T cells were enriched in the presence of TGF-β1 alone (44.6% ± 1.0%) (Fig. 4c). The combination of CRCs and TGF-β1 (28.9% ± 2.7%) was lower than TGF-β1 alone, but similar to the Dynabead-only and DMSO controls.

CRCs preferentially enrich CD4$^+$CD25$^+$FoxP3$^+$ primary human T cells

We next tested the Rapa concentration-dependent enrichment of CD4$^+$CD25$^+$FoxP3$^+$ human T_{reg} with DMSO-solubilized Rapa. T cells were enriched from donor derived PBMCs using magnetic depletion to a purity of approximately 85% CD8$^+$ and CD4$^+$ T cells (Fig. S1c†) and subsequently activated using Dynabeads. The suppression in hT cell expansion was similar at 1 μM (8.84 ± 0.62-fold), 100 nM (8.88 ± 2.72-fold), and 10 nM (8.92 ± 1.41-fold) DMSO-solubilized Rapa, relative to the Dynabead-only control (24.5 ± 3.8-fold) (Fig. 5a and b). The enrichment in CD4$^+$CD25$^+$FoxP3$^+$ human T_{reg} at 1 μM (22.1% ±

1.7%), 100 nM (22.2% ± 0.81%), and 10 nM Rapa (21.3% ± 1.3%) was similar and greater than the Dynabead-only control (12.0% ± 2.2%) (Fig. 5c).

To test the bioactivity of CRCs with hT cells, we measured CRC-mediated suppression on hT cell expansion with 1 μM, 100 nM, and 10 nM CRCs (Fig. 5d). At 10 nM, T cell expansion was comparable to the Dynabead-only control (23.8 ± 2.5-fold expansion) as well as the βCD-NH$_2$ control (25.0 ± 2.7-fold expansion). However, at 100 nM (8.7 ± 1.2-fold) and 1 μM CRC (7.7 ± 0.6-fold), suppression in T cell expansion was comparable to DMSO-solubilized 100 nM Rapa (9.0 ± 0.6-fold) (Fig. 5e). Similarly, the enrichment of CD4$^+$CD25$^+$FoxP3$^+$ T_{regs} at 10 nM CRCs (12.0% ± 1.2%) was comparable to the Dynabead-control (14.1% ± 1.6%) and βCD-NH$_2$ control (14.5% ± 1.5%). Enrichment at 100 nM (21.8% ± 1.2%) and 1 μM (21.4% ± 1.4%) CRCs was higher than the Dynabead-control and comparable to 100 nM DMSO-solubilized Rapa (22.3% ± 1.9%) (Fig. 5f).

Expansion with TGF-β1 and CRCs results in high fraction of CD4$^+$CD25$^+$FoxP3$^+$ hT cells

To test the effect of TGF-β1 in combination with CRCs on T_{reg} enrichment we cultured PBMC-derived hT cells with the same single-factor and combination treatments previously described for murine T cells (Fig. 6a). CRCs in combination with TGF-β1
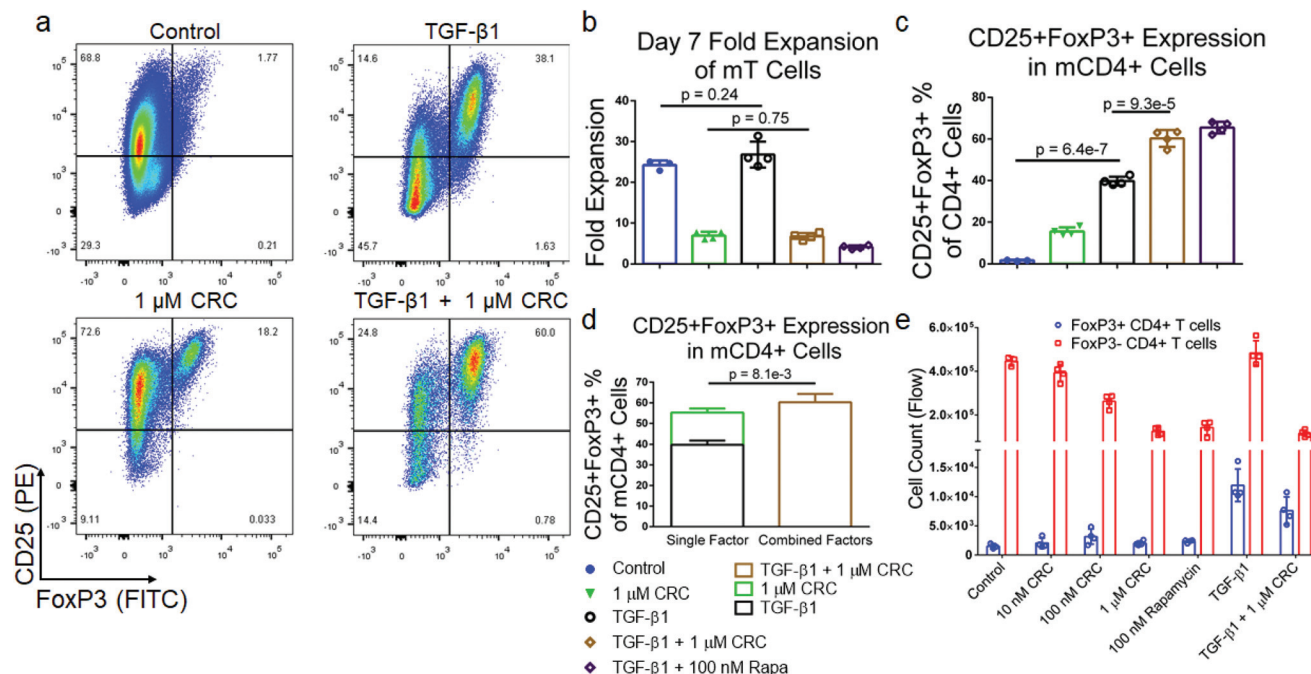
Fig. 3 Mouse T_{regs} are enriched with combination of TGF-β1 and CRCs. (a) Representative flow cytometry plots gated on $CD4^+CD25^+FoxP3^+$ mT cells with TGF-β1, CRCs or both. Quantification of the fold expansion of splenic $CD4^+$ and $CD8^+$ T cells (b) and the fraction of $CD25^+FoxP3^+$ $CD4^+$ T cells (c) after 7 days of expansion. (d) Stacked columns representative of the additive enrichment in the fraction of $CD25^+FoxP3^+$ $CD4^+$ T cells mediated with single-factor TGF-β1 (black) and CRCs (green) compared to the enrichment with combination TGF-β1 and CRCs (brown). (e) Quantification of $CD4^+FoxP3^+$ and $CD4^+FoxP3^-$ T cells with CRCs and TGF-β1. In a–e, untreated, TGF-β1, CRCs, TGF-β1 and CRCs, and TGF-β1 and Rapa were compared. Data represents the mean ± s.d. (n = 4). Experiments were repeated at least two times.

(3.2 ± 0.4-fold expansion) suppressed hT cell proliferation more than CRCs (5.3 ± 1.2-fold expansion) or TGF-β1 (22.3 ± 0.4-fold expansion) alone (Fig. 6b). The fraction of $CD25^+FoxP3^+$ T cells among $CD4^+$ T cells was highest in the combination group (63.5% ± 7.4%), though the enrichment was not greater than the single treatment CRCs (58.1% ± 2.7%) and TGF-β1 (32.9% ± 0.6%) combined (Fig. 6c).

TGF-β1 and CRCs reduce IFNγ expression, enrich IFNγ⁻TNFα⁺ human T cells

To characterize the effect of CRCs on cytokine expression in hT cells alone and in combination with TGF-β1, we expanded T cells as previously described. After 7 days of expansion, the cells were re-stimulated with phorbol 12-myristate 13-acetate (PMA) and ionomycin and analyzed for interferon-γ (IFNγ) and tumor necrosis factor-α (TNFα) expression (Fig. 7a and b). DMSO-solubilized 100 nM Rapa (8.1% ± 0.4%) and 1 μM CRCs (8.6% ± 0.5%) reduced IFNγ expression of $CD4^+$ hT cells relative to a DMSO-treated control (14.7% ± 1.1%) and untreated control (12.4% ± 1.1%) (Fig. 7c). TGF-β1 alone (11.3% ± 0.4%) did not reduce IFNγ relative to controls. However, TGF-β1 in combination with 1 μM CRCs (5.2% ± 0.3%) decreased IFNγ more than TGF-β1 or 1 μM CRCs alone. TGF-β1 (49.5% ± 1.6%) increased the fraction of IFNγ⁻TNFα⁺ more than the combination of 1 μM CRCs and TGF-β1 (46.0% ± 0.7%) relative to untreated control (31.5% ± 4.8%) (Fig. 7d). DMSO-solubilized 100 nM Rapa (34.6% ± 4.3%) did not increase the IFNγ⁻TNFα⁺

fraction relative to DMSO containing controls (31.9% ± 1.5%), while 1 μM CRCs (39.6% ± 2.9%) enhanced the fraction relative to control.

Computational model characterizes the dependence of T_{reg} enrichment to initial cell population

To explain how culture conditions and starting cell populations contribute to experimental outcomes and variance, we developed and optimized a model describing the kinetics of differentiation and expansion of model naïve (T_n), regulatory (T_r) and effector (T_e) $CD4^+$ T cells (Fig. 8a). Details of the model and parameter fitting may be found in the ESI.† First, we looked at the sensitivity to the initial T_r population over a range of commonly reported T_{reg} splenocyte fractions. We initialized the model with 1%, 2%, and 3% T_r with a fixed T_e (36.5%) fraction and variable T_n (62.5%, 61.5% and 60.5%) fraction that correspond to the averages of values from isolated murine splenocytes analyzed via flow cytometry (Fig. S1d†). This revealed that the post-expansion T_r fraction was most sensitive to the initial T_r fraction in the 1 μM CRC condition with a range of 4.9%–13.8%, while outcomes for control (3.0%–8.7%), TGF-β1 (39.7%–42.2%), and combination (53.1%–55.6%) conditions are tightly grouped and independent of the initial T_r fraction (Fig. 8b). The results from the model were consistent with experimental data for control (5.80% ± 1.66% vs. 2.61% ± 1.03%), 1 μM CRC (9.38% ± 2.58% vs. 12.6% ± 5.9%), and TGF-β1 (39.1% ± 6.1% vs. 34.6% ± 6.3%), and
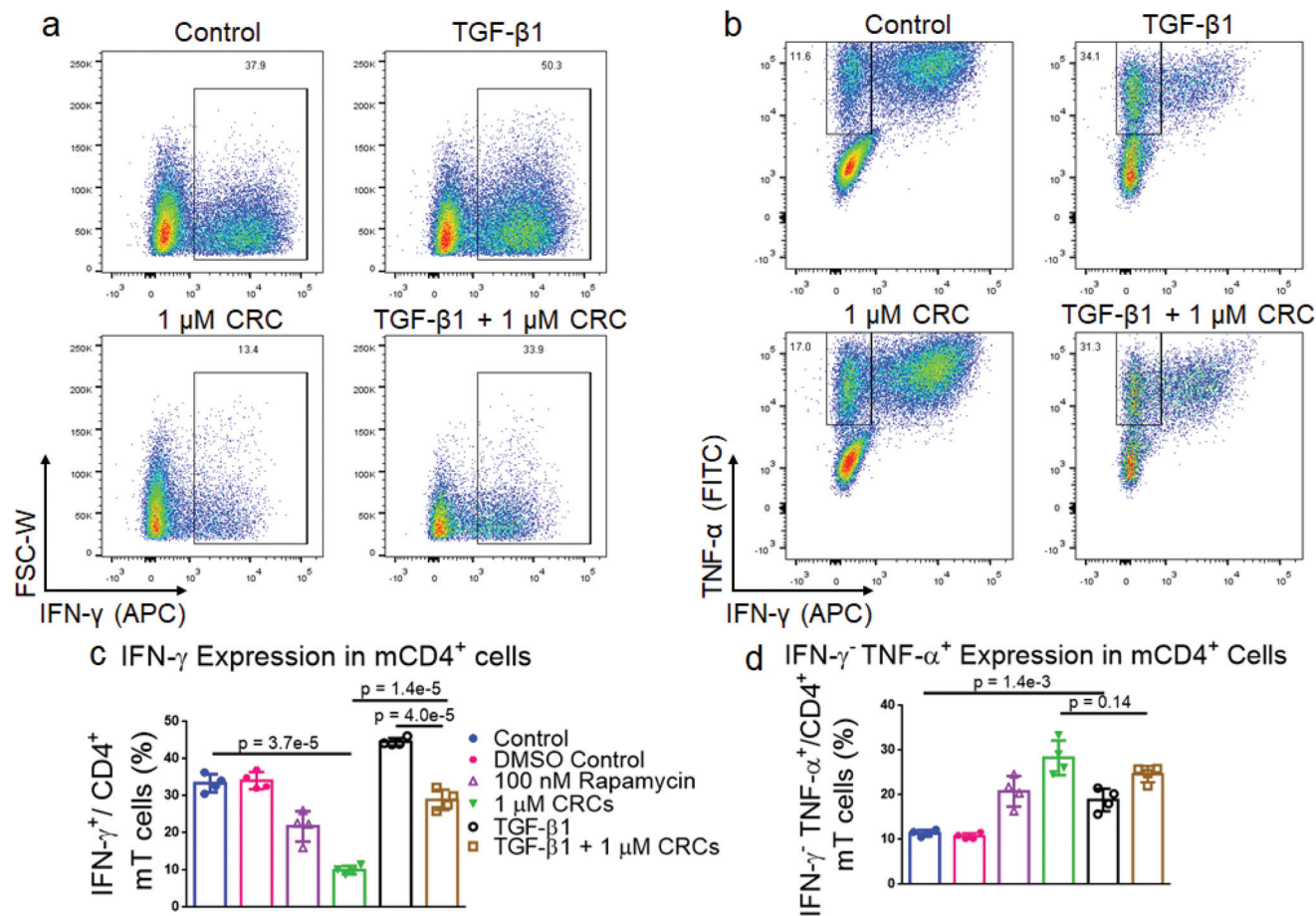
Fig. 4 CRCs and TGF-β1 modulate cytokine expression in CD4+ murine T cells. Representative flow cytometry plots showing the fraction of IFN-γ+ (a) and INF-γ−TNF-α+ (b) CD4+ mT cells when TGF-β1, CRCs or both are included in culture medium. Flow cytometry of IFN-γ+ (c) and INF-γ−TNF-α+ (d) CD4+ T cells after 7 days of expansion. In a−d, untreated cells, TGF-β1, CRCs, TGF-β1 and CRCs, and TGF-β1 and Rapa were compared. Data represents the mean ± s.d. (n = 4). Experiments were repeated at least two times.

slightly underestimated T_r enrichment by the combination of CRC/TGF-β1 (52.2% ± 6.5% *vs.* 62.7% ± 4.2%), but still demonstrated a synergistic effect (Fig. 8c). Due to the high variability in naïve T cell fraction in human peripheral blood samples, we next analyzed the sensitivity of final T_r fraction to the initial naïve-to-effector T cell ratio. We quantified the effect of changing the initial T_e fraction between 18.2%, 36.5% and 54.7% while fixing the T_r fraction at 2%. The range of values for the initial T_e fraction was chosen to cover the range of observed fractions of effector T cells seen in human and mouse samples. The impact of variance in initial T_e fraction on the final T_r fraction was significantly higher with TGF-β1 (27.4%–47.3%) and combination of CRC/TGF-β1 (39.4%–60.5%), and minimal in the control (5.5%–6.1%) and with CRCs only (9.0%–9.7%) (Fig. 8d). Finally, to characterize the role that the delay in hT cell expansion kinetics relative to mT cells plays in abrogating the synergistic effect of combination CRC/TGF-β1, a modified model was used in which expansion did not begin until 48 hours after differentiation. Results from the modified model revealed that the additive T_{reg} enrichment observed with 1 μM CRCs (7.86% ± 2.35%) or TGF-β1 (36.8% ± 5.3%)

alone was not significantly different than the combination of both factors (45.6% ± 5.6%) (Fig. 8e).

Discussion

Here we demonstrate T_{regs} are enriched up to 5-fold *in vitro* in which β-cyclodextrin encapsulated Rapa complex (CRC) plays a key role in the differential modulation of proliferating T cell subsets. The encapsulation of Rapa in the CRC enhanced its activity *in vitro* and delivery to T cells, synergizing with TGF-β1 to efficiently produce mouse and human T_{regs}. Encapsulation of Rapa in the CRC by equilibrium mixing was directly proportional to the concentration of the βCD-NH2 concentration, up to the limit of solubility of βCD-NH2. The CRC complex significantly improved the aqueous solubility of Rapa by over 2 orders of magnitude and was stable in solution for at least one month. The addition of CRCs in T cell growth medium selectively suppressed the expansion of CD4+FoxP3− T cells in a dose-dependent manner and enhanced the fraction of CD4+FoxP3+ T_{regs} with both mT and hT cells. The coadminis-
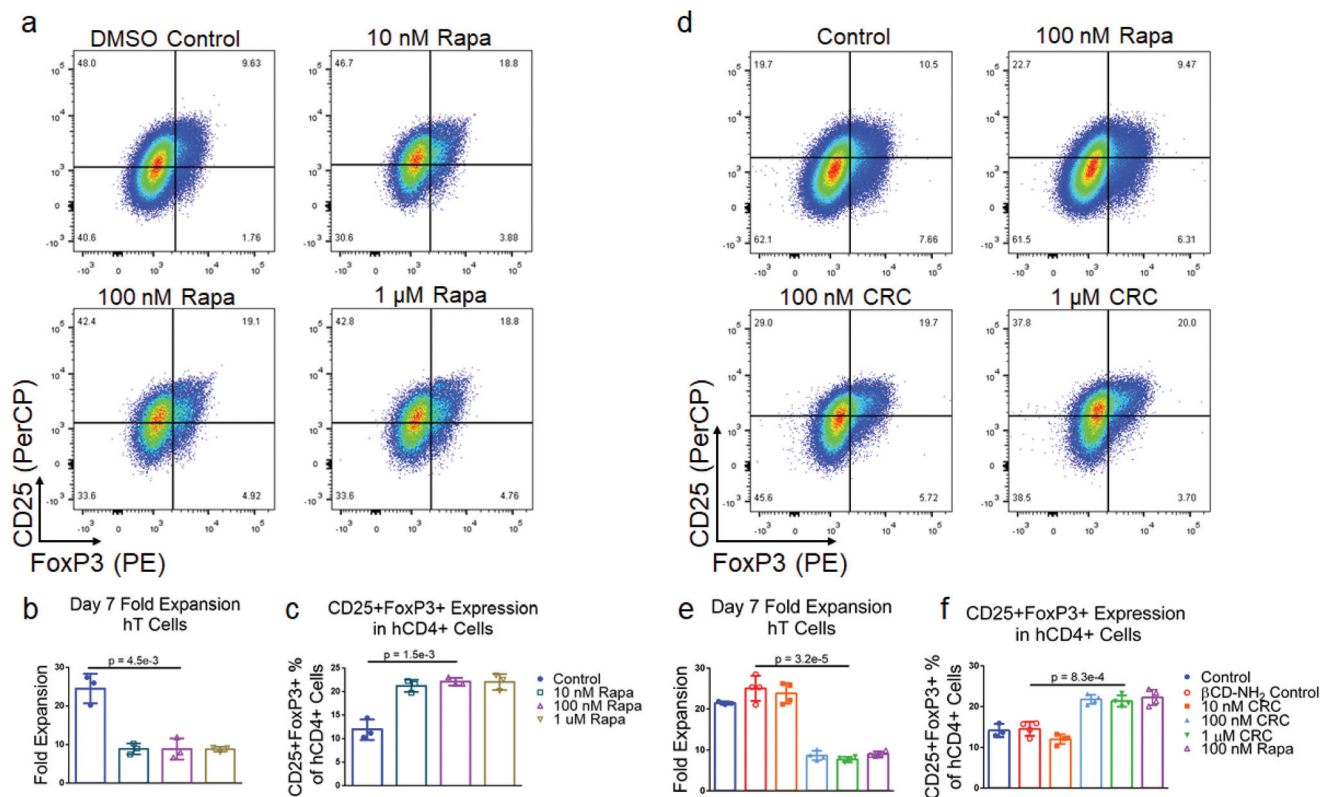
Fig. 5 Rapa and CRCs suppress human T cell expansion and enhances human T_{reg}. (a) Representative flow cytometry of CD4$^+$CD25$^+$FoxP3$^+$ human T (hT) cells when Rapa is include in the culture medium. Quantification of the fold expansion of CD4$^+$ and CD8$^+$ T cells (b) and the fraction of CD4$^+$CD25$^+$FoxP3$^+$ T cells (c) after 7 days of expansion with varying concentrations of Rapa. (d) Representative flow cytometry of CD4$^+$ CD25$^+$FoxP3$^+$ T cells when CRCs are included in culture medium. Quantification of the fold expansion of CD4$^+$ and CD8$^+$ T cells (e) and the fraction of CD25$^+$FoxP3$^+$ CD4$^+$ T cells (f) after 7 days of expansion with multiple concentrations of CRCs. Data represents the mean ± s.d. (n = 4). Experiments were repeated at least three times.

tration of the T cell modulating factor TGF-β1 and CRC enriched mouse and human T_{regs} through the expansion of CD4$^+$FoxP3$^+$ T_{regs} and suppression of CD4$^+$FoxP3$^-$ T cells respectively, with evidence of synergism in mouse T_{reg} expansion. The findings are consistent with the observations of CRC-mediated reduction in the expression of the inflammatory mediator, IFN-γ, in both mT and hT cells.

Mono-(6-amino-6-deoxy)-beta-cyclodextrin enhances the aqueous solubility of Rapa over 100-fold and is a stable carrier for Rapa. Mono-(6-amino-6-deoxy)-beta-cyclodextrin was chosen as it has significantly enhanced solubility compared to unmodified beta-cyclodextrin and previous reports found that hydroxypropyl-beta-cyclodextrin minimally improved Rapa solubility.[32] The ~1 : 100 ratio of solubilized Rapa to βCD-NH$_2$s is comparable to Rapa encapsulation with other βCD molecules. After an initial decrease in concentration βCD-NH$_2$-Rapa complexes maintained a stable concentration in solution and retained their bioactivity for up to one month (Fig. S3†). The initial drop in concentration is likely due to the small fraction that dissociates to establish equilibrium.

The CRCs potently modulated both mT and hT cells, supporting the relevance of this delivery strategy for Rapa in generating T_{regs} *in vitro*. In prior work, particle systems composed

of poly(lactide-*co*-glycolide) (PLGA), poly(D,L-lactide) (PDLLA), poly(ε-caprolactone) (PCL), and poly(alkyl cyanoacrylates) (PACs) have been used to improve the bioavailability of Rapa *in vivo* and improved its delivery to target tissues before release.[12,33,34] However, in contrast to *in vivo* delivery, particle-based Rapa delivery systems are unsuitable for *in vitro* expansion as their uptake by activated T cells is highly inefficient. Moreover, the high concentration of degradable synthetic polymers *in vitro* would likely be cytotoxic. The introduction of synthetic polymers would also increase the complexity of manufacturing *in vitro* generated T_{regs}.

The apparent effect of Rapa in the CRC was diminished by approximately 100-fold in mT cells and 10-fold in hT cells compared to DMSO-solubilized Rapa. In contrast to cyclodextrins, DMSO is a cell membrane permeabilizing agent that directly inserts and disrupts the cell membrane and thereby facilitates intracellular drug delivery. However, the use of DMSO for intracellular delivery is not a scalable strategy for T cell manufacturing *in vitro*. Consistent with prior results, we observe that CD4$^+$ T cells are highly sensitive to the concentration of DMSO and even low doses potently suppresses their expansion.[35] Moreover, DMSO are potentially toxic at the high concentrations that are often used to manufacture cells, which
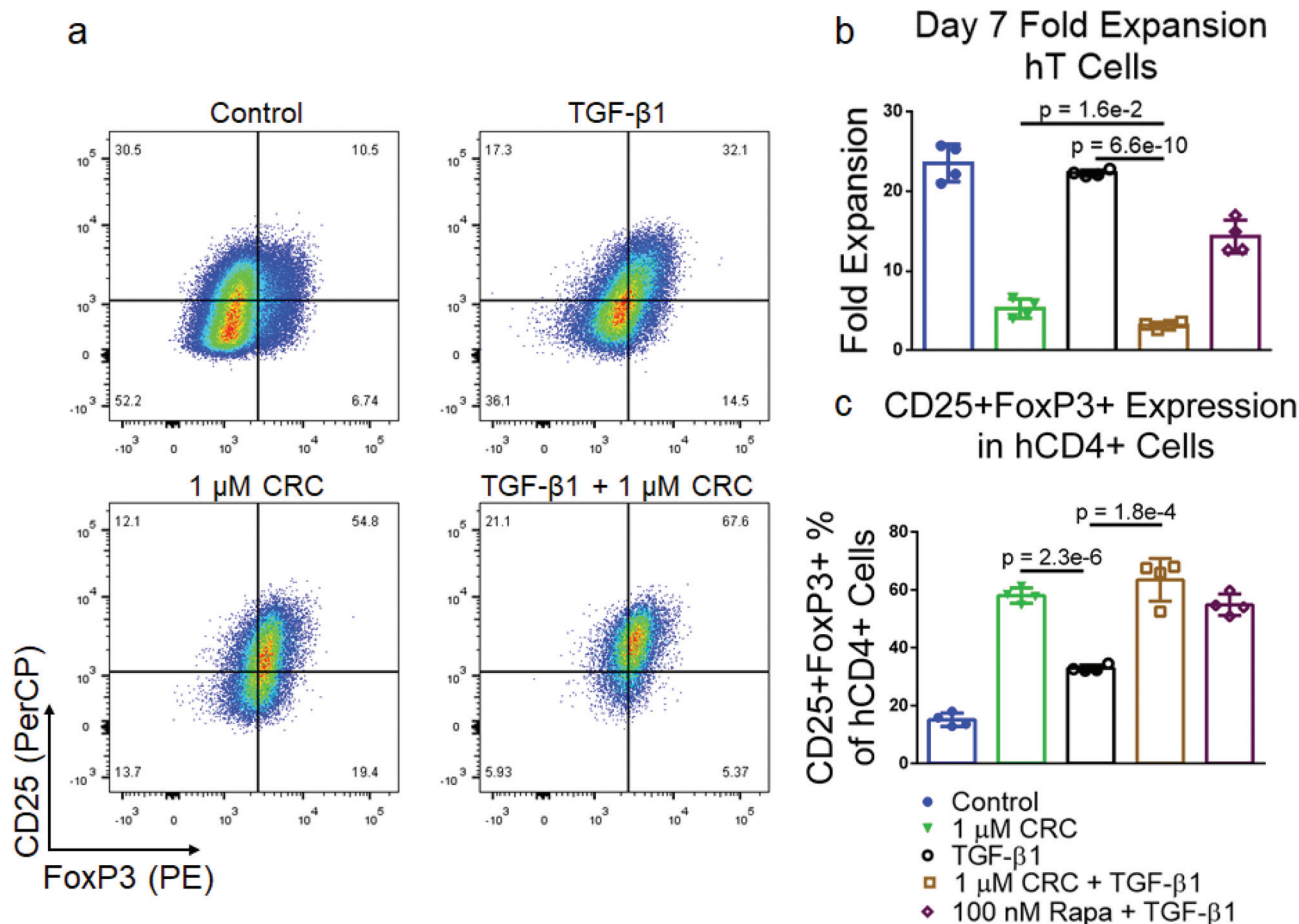
Fig. 6 Human T_{regs} are enriched with the combination of TGF-β1 and CRCs. (a) Representative flow cytometry of CD25$^+$FoxP3$^+$ CD4$^+$ T cells when TGF-β1, CRCs or both are included in culture media. Quantification of the fold expansion of splenic CD4$^+$ and CD8$^+$ T cells (b) and the fraction of CD4$^+$CD25$^+$FoxP3$^+$ T cells (c) after 7 days of expansion. In a–c, untreated cells, TGF-β1, CRCs, TGF-β1 and CRCs, and TGF-β1 and Rapa were analyzed. Data represents the mean $\pm$ s.d. (n = 4). Experiments were repeated at least two times.

complicates direct use in patients, and its removal is a complex processes associated with a detrimental osmotic shock to the cells.[36] In contrast, and consistent with prior reports, we observe that T cell growth, function and phenotype is not affected by βCD-NH$_2$ alone.

The difference in the intracellular concentration of Rapa may have a considerable effect on the enrichment of T_{regs} because of the concentration-dependent effect on mTOR complex formation (mTORC1 and mTORC2). We observed that the suppression in mT cell expansion was dose dependent for 10 nm, 100 nm, and 1 μM CRC, while enrichment in T_{reg} was observed for 1 μM CRC. These findings are consistent with previous reports, which have established that mTORC1 is more sensitive to Rapa-mediated inhibition than mTORC2.[37] Inhibition of mTORC1 prevents the differentiation of T helper (Th) 1 CD4$^+$ T cells, consistent with the reduction of IFN-γ expression of T cells expanded with CRCs, and is an important step for enriching T_{reg}[38] On the other hand, the inhibition of mTORC2 enhances the suppressive capacity of T_{reg}.[39] Robust mTORC2 inhibition requires sustained exposure to higher concentrations of Rapa, and therefore CRCs are preferred over

DMSO as they are an inert carrier and preserve bioactivity of Rapa, and thereby sustain presentation to T cells.[40]

The enhancement in murine T_{regs} with CRCs together with TGF-β1 was greater than the sum of T_{regs} when either factor was applied individually. CRCs increased the fraction T_{regs} primarily *via* suppression of CD4$^+$CD25$^+$FoxP3$^-$ T cell expansion whereas TGF-β1 increased the fraction of T_{regs} by increasing the absolute number of CD4$^+$CD25$^+$FoxP3$^+$ T cells. This observation is supported by prior observations of the synergistic effect of Rapa and TGF-β1 for the *in vitro* induction of T_{regs} from naïve CD4$^+$ T cells. The *in vitro* enhancement of human T_{regs} from naïve T cells by TGF-β1 alone is consistent with prior reports. However, in contrast to splenocyte-isolated mT cells, naïve CD4$^+$ T cells must be isolated from human blood and only make up 1–10% of leukocytes, with significant variation between donors. This variability supports the combined use of both Rapa and TGF-β1 to generate human T_{reg}. Here, we confirmed that the immunomodulation by Rapa and TGF-β1 extends to polyclonal T cells, consisting of both mature and naïve T cells (Fig. S1d†). The enhancement of the T_{reg} from heterogenous T cell subsets is clinically relevant as PBMC-iso-
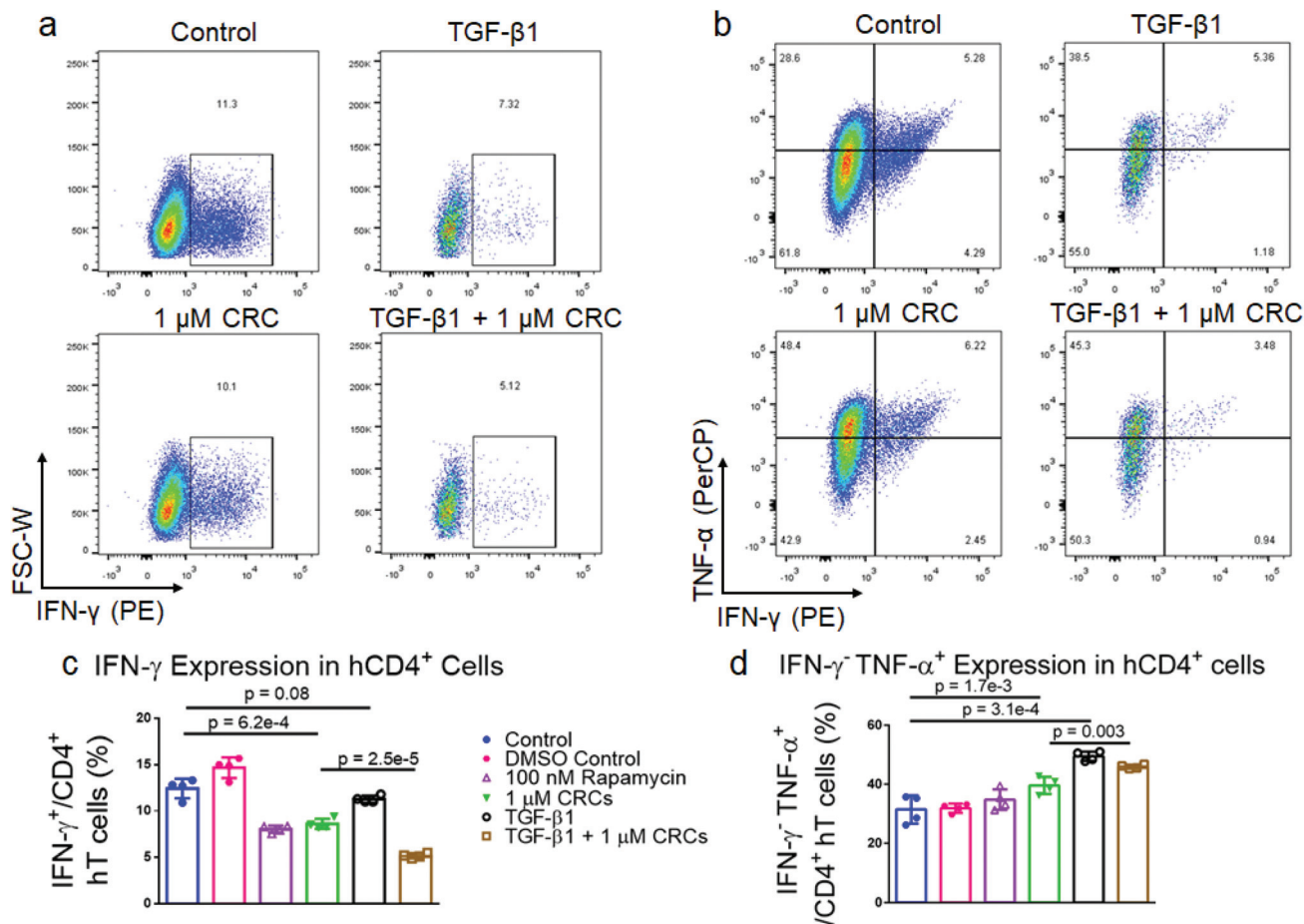
Fig. 7 CRCs and TGF-β1 modulate cytokine expression in CD4^{+} human T cells. Representative flow cytometry of IFN-γ^{+} (a) and INF-γ^{−}TNF-α^{+} (b) CD4^{+} T cells when TGF-β1, CRCs or both are included in culture media. Flow cytometry of IFN-γ^{+} (c) and INF-γ^{−}TNF-α^{+} (d) CD4^{+} T cells after 7 days of expansion. In a−d, untreated cells, TGF-β1, CRCs, TGF-β1 and CRCs, and TGF-β1 and Rapa were compared. Data represents the mean ± s.d. (n = 4). Experiments were repeated at least two times.

lated T cells are often a combination of memory T cells and recently activated naïve T cells.

The reduction in IFNγ expression and enrichment of IFNγ[−]TNFα[+] mediated by CRCs was consistently observed in both mT and hT cells. In mT cells, TGF-β1 enhanced the expression of both IFNγ and TNFα. This is consistent with prior reports characterizing the inhibition of naïve murine T cell activation and enhancement of Th1 cells in a mixed T cell population by TGF-β1.[41] Because the initially isolated T cells contained a mixed population of T cell subsets, the TGF-β1 likely enhanced activation of pre-existing Th1 T cells. In contrast, with hT cells, the combination of TGF-β1 and CRCs decreased the fraction of IFNγ^{+} T cells more than either factor individually. The difference in cytokine expression between mT and hT cells suggests that the source of T cells for T_{reg} enrichment is important. Furthermore, TGF-β1 did not enhance IFN-γ expression in hT cells and supports the translation of this approach for T_{reg} expansion in the clinic, where it will likely be difficult to enrich high numbers of naïve autologous T cells. CRCs enhanced the fraction of IFN-γ[−]TNF-α^{+} T cells. This observation is consistent with prior reports that

have demonstrated that T_{reg} priming *via* the TNFRII receptor enhances T_{reg} function and TNFRII marks a highly immunosuppressive T_{regs} subset.[42]

The kinetic growth model describing T_{reg} expansion and differentiation supported the role of CRCs in mediating T_{reg} enrichment primarily through suppression of effector T cell expansion, and that of TGF-β1 through the differentiation of naïve T cells into T_{regs}. Strikingly, the model accurately recapitulates the synergistic effect of CRCs and TGF-β1 in murine T cells, and the incorporation of a delay in T cell expansion abrogates this effect, providing a possible explanation for why synergism is not observed under the same conditions with hT cells. However, the model under-represents the fraction of T_{regs} in the murine combination condition, and in human control and CRC only conditions. CRCs inhibit IFN-γ, a key driver of Th1 differentiation. Thus, in the combination conditions the rate of differentiation into effector CD4 T cells is likely lower than predicted by the model, and a larger fraction differentiates into T_{regs}. The model is also useful for evaluating the distribution of final T cell subsets based on the initial fractions and suggests that a high naïve-to-effector ratio improves the
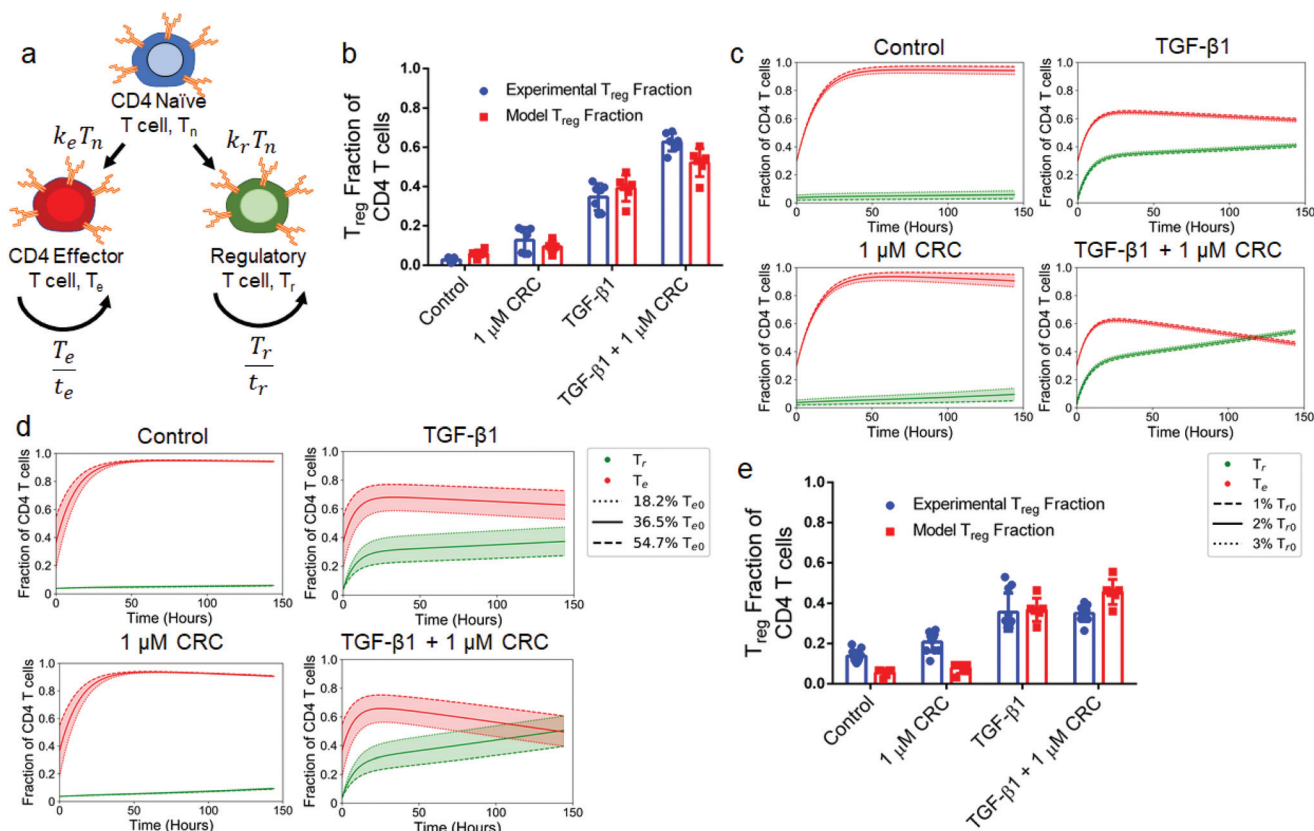
Fig. 8 Enrichment of T$_{reg}$ *in vitro* is enhanced with a high initial naïve-to-effector T cell ratio. (a, b) Schematic depicting the interactions between T cells in a model of T cell expansion (a) and side-by-side comparison of experimental data (red) and model predictions (blue) when of TGF-β1, CRCs, both, or neither (Control) are included in culture media (b). (c) Model predictions for the fraction of effector (red) and regulatory (green) T cells when simulations are initialized with 1%, 2% or 3% T$_{reg}$ in the starting population corresponding to the dashed, solid, and dotted lines respectively. (d) Model predictions for the fraction of effector (red) and regulatory (green) T cells when simulations are initialized with 54.7%, 36.5% or 18.2% effector T cells in the starting population corresponding to the dashed, solid, and dotted lines respectively. (e) Predictions for effector and regulatory T cell fractions when a two day delay is placed on T cell expansion to mimic hT cell expansion dynamics. In b, experimental data represents the mean ± s.d. (*n* = 7) and model data represents the final values for the three simulations depicted in (c).

enrichment of T$_{reg}$, confirming the importance of pre-sorting for naïve T cells before expansion and phenotypic modulation in clinical applications.[43] As quality control guidelines for ACT based T$_{reg}$ therapies are established, this model may serve as the basis for a tool to determine product sensitivity to key input parameters and apply process controls to minimize variance in T$_{reg}$ manufacturing, a necessary step in developing good manufacturing practice protocols.[44]

Conclusions

Our findings collectively suggest that the βCD-NH$_2$ encapsulated Rapa enhances T$_{reg}$ *in vitro*. CRCs increase the bioavailability of Rapa due to strong hydrophobic interactions with βCD-NH$_2$, and the stability of the inclusion complex was confirmed *via* spectrophotometry. Compared with DMSO, the CRCs (i) improve the solubility of Rapa without inducing T cell toxicity, (ii) shield Rapa from degradation, thereby increasing half-life and uptake by T cells, (iii) synergize with TGF-β1 to enhance preferential expansion of T$_{reg}$. Additionally, CRCs sig-

nificantly decrease the production of IFN-γ by effector T cells and thereby reduces naïve T cells differentiation into a Th1 phenotype. The enhancement in TNF-α expression may act to prime the T$_{regs}$ and enhance functionality. The kinetic model recapitulates the synergism between the CRCs and TGF-β1 in modulating the kinetics of T$_{reg}$ expansion *in vitro* and evaluates parameters for scalable manufacturing methods for immune cell therapies with T$_{reg}$.

While the current study investigated enhancement of polyclonal T$_{reg}$ *in vitro*, further development of CRCs in combination with TGF-β1 for *in vivo* local delivery could enable the enhancement of T$_{reg}$ for a number of local and systemic autoimmune diseases. Given that Rapa and TGF-β1 are clinically used therapies, their application for immune cell manufacturing could enable safer administration of T$_{reg}$ as a means to treat autoimmune disease either alone or in combination with therapeutics currently utilized in the clinic. It may be a means of abrogating the significant side effects that limit clinical application of these pleiotropic drugs by restricting their potent immunomodulatory effects to T cells.

Author contributions

D. A. M., M. D. K. and N. J. S., conceived the ideas, designed the experiments, analyzed and interpreted the data and wrote the manuscript. D. A. M., M. D. K., S. L. W., Y. Y. Y., and D. A. O., conducted the experiments. All authors discussed the results and provided input in writing the manuscript.

Conflicts of interest

The authors have no relevant competing financial interests or relationships that could have influenced the work reported in this paper.

Acknowledgements

References

1 S. Sakaguchi, R. Setoguchi, H. Yagi and T. Nomura, *Curr. Top. Microbiol. Immunol.*, 2006, **305**, 51–66.

2 J. A. Bluestone and Q. Tang, *Science*, 2018, **362**, 154–155.

3 N. Marek-Trzonkowska, M. Mysliwiec, A. Dobyszuk, M. Grabowska, I. Derkowska, J. Juscinska, R. Owczuk, A. Szadkowska, P. Witkowski, W. Mlynarski, P. Jarosz-Chobot, A. Bossowski, J. Siebert and P. Trzonkowski, *Clin. Immunol.*, 2014, **153**, 23–30.

4 G. P. Wright, C. A. Notley, S. A. Xue, G. M. Bendle, A. Holler, T. N. Schumacher, M. R. Ehrenstein and H. J. Stauss, *Proc. Natl. Acad. Sci. U. S. A.*, 2009, **106**, 19078–19083.

5 N. J. Shah, A. S. Mao, T. Y. Shih, M. D. Kerr, A. Sharda, T. M. Raimondo, J. C. Weaver, V. D. Vrbanac, M. Deruaz, A. M. Tager, D. J. Mooney and D. T. Scadden, *Nat. Biotechnol.*, 2019, **37**, 293–302.

6 B. R. Olden, C. R. Perez, A. L. Wilson, I. I. Cardle, Y. S. Lin, B. Kaehr, J. A. Gustafson, M. C. Jensen and S. H. Pun, *Adv. Healthcare Mater.*, 2019, **8**, e1801188.

7 C. S. Verbeke, S. Gordo, D. A. Schubert, S. A. Lewin, R. M. Desai, J. Dobbins, K. W. Wucherpfennig and D. J. Mooney, *Adv. Healthcare Mater.*, 2017, **6**, 1600773.

8 Q. Tang, K. J. Henriksen, M. Bi, E. B. Finger, G. Szot, J. Ye, E. L. Masteller, H. McDevitt, M. Bonyhadi and J. A. Bluestone, *J. Exp. Med.*, 2004, **199**, 1455–1465.

9 A. L. Putnam, T. M. Brusko, M. R. Lee, W. Liu, G. L. Szot, T. Ghosh, M. A. Atkinson and J. A. Bluestone, *Diabetes*, 2009, **58**, 652–662.

10 S. Sakaguchi, K. Wing, Y. Onishi, P. Prieto-Martin and T. Yamaguchi, *Int. Immunol.*, 2009, **21**, 1105–1111.

11 J. Li, S. G. Kim and J. Blenis, *Cell Metab.*, 2014, **19**, 373–379.

12 A. Haeri, M. Osouli, F. Bayat, S. Alavi and S. Dadashzadeh, *Artif. Cells, Nanomed., Biotechnol.*, 2018, **46**, 1–14.

13 N. Saber-Moghaddam, H. Nomani, A. Sahebkar, T. P. Johnston and A. H. Mohammadpour, *Int. Immunopharmacol.*, 2019, **69**, 150–158.

14 Y. Dobashi, Y. Watanabe, C. Miwa, S. Suzuki and S. Koyama, *Int. J. Clin. Exp. Pathol.*, 2011, **4**, 476.

15 M. Battaglia, A. Stabilini, B. Migliavacca, J. Horejs-Hoeck, T. Kaupper and M. G. Roncarolo, *J. Immunol.*, 2006, **177**, 8338–8347.

16 P. Monti, M. Scirpoli, P. Maffi, L. Piemonti, A. Secchi, E. Bonifacio, M. G. Roncarolo and M. Battaglia, *Diabetes*, 2008, **57**, 2341–2347.

17 H. Q. Niu, Z. H. Li, W. P. Zhao, X. C. Zhao, C. Zhang, J. Luo, X. C. Lu, C. Gao, C. H. Wang and X. F. Li, *Clin. Exp. Rheumatol.*, 2019, **38**, 58–66.

18 A. Schmidt, M. Eriksson, M. M. Shang, H. Weyd and J. Tegner, *PLoS One*, 2016, **11**, e0148474.

19 M. Esposito, F. Ruffini, M. Bellone, N. Gagliani, M. Battaglia, G. Martino and R. Furlan, *J. Neuroimmunol.*, 2010, **220**, 52–63.

20 H.-J. Shin, J. Baker, D. B. Leveson-Gower, A. T. Smith, E. I. Sega and R. S. Negrin, *Blood*, 2011, **118**, 2342–2350.

21 K. Wieder, W. Hancock, G. Schmidbauer, C. Corpier, I. Wieder, L. Kobzik, T. Strom and J. Kupiec-Weglinski, *J. Immunol.*, 1993, **151**, 1158–1166.

22 R. Setoguchi, Y. Matsui and K. Mouri, *Eur. J. Immunol.*, 2015, **45**, 893–902.

23 K. Mahalati and B. D. Kahan, *Clin. Pharmacokinet.*, 2001, **40**, 573–585.

24 P. Simamora, J. M. Alvarez and S. H. Yalkowsky, *Int. J. Pharm.*, 2001, **213**, 25–29.

25 M. E. Davis and M. E. Brewster, *Nat. Rev. Drug Discovery*, 2004, **3**, 1023.

26 F. Hirayama and K. Uekama, *Adv. Drug Delivery Rev.*, 1999, **36**, 125–141.

27 V. J. Stella and Q. He, *Toxicol. Pathol.*, 2008, **36**, 30–42.

28 M. A. Rouf, I. Vural, E. Bilensoy, A. Hincal and D. D. Erol, *J. Inclusion Phenom. Macrocyclic Chem.*, 2011, **70**, 167–175.

29 Y. Dou, J. W. Guo, Y. Chen, S. L. Han, X. Q. Xu, Q. Shi, Y. Jia, Y. Liu, Y. C. Deng, R. B. Wang, X. H. Li and J. X. Zhang, *J. Controlled Release*, 2016, **235**, 48–62.

30 N. A. Rohner, S. J. Schomisch, J. M. Marks and H. A. von Recum, *Mol. Pharmaceutics*, 2019, **16**, 1766–1774.

31 S. Yamagiwa, J. D. Gray, S. Hashimoto and D. A. Horwitz, *J. Immunol.*, 2001, **166**, 7282–7289.

32 M.-S. Kim, J.-S. Kim, H. J. Park, W. K. Cho, K.-H. Cha and S.-J. Hwang, *Int. J. Nanomed.*, 2011, **6**, 2997.

33 J. Zhao, Z. Mo, F. Guo, D. Shi, Q. Q. Han and Q. Liu, *J. Biomed. Mater. Res., Part B*, 2018, **106**, 88–95.

34 S. Jhunjhunwala, S. C. Balmert, G. Raimondi, E. Dons, E. E. Nichols, A. W. Thomson and S. R. Little, *J. Controlled Release*, 2012, **159**, 78–84.

35 L. Holthaus, D. Lamp, A. Gavrisan, V. Sharma, A.-G. Ziegler, M. Jastroch and E. Bonifacio, *J. Immunol. Methods*, 2018, **463**, 54–60.

36 S. Thirumala, W. S. Goebel and E. J. Woods, *Organogenesis*, 2009, **5**, 143–154.

37 A. Toschi, E. Lee, L. Xu, A. Garcia, N. Gadir and D. A. Foster, *Mol. Cell. Biol.*, 2009, **29**, 1411–1420.

38 G. M. Delgoffe, K. N. Pollizzi, A. T. Waickman, E. Heikamp, D. J. Meyers, M. R. Horton, B. Xiao, P. F. Worley and J. D. Powell, *Nat. Immunol.*, 2011, **12**, 295–303.

39 L. M. Charbonnier, Y. Cui, E. Stephen-Victor, H. Harb, D. Lopez, J. J. Bleesing, M. I. Garcia-Lloret, K. Chen, A. Ozen, P. Carmeliet, M. O. Li, M. Pellegrini and T. A. Chatila, *Nat. Immunol.*, 2019, **20**, 1208–1219.

40 D. D. Sarbassov, S. M. Ali, S. Sengupta, J. H. Sheen, P. P. Hsu, A. F. Bagley, A. L. Markhard and D. M. Sabatini, *Mol. Cell*, 2006, **22**, 159–168.

41 D. J. Huss, R. C. Winger, H. Peng, Y. Yang, M. K. Racke and A. E. Lovett-Racke, *J. Immunol.*, 2010, **184**, 5628–5636.

42 X. Chen, J. J. Subleski, H. Kopf, O. Z. Howard, D. N. Männel and J. J. Oppenheim, *J. Immunol.*, 2008, **180**, 6467–6471.

43 J. M. Marin Morales, N. Munch, K. Peter, D. Freund, U. Oelschlagel, K. Holig, T. Bohm, A. C. Flach, J. Kessler, E. Bonifacio, M. Bornhauser and A. Fuchs, *Front. Immunol.*, 2019, **10**, 38.

44 S. Eaker, M. Armant, H. Brandwein, S. Burger, A. Campbell, C. Carpenito, D. Clarke, T. Fong, O. Karnieli, K. Niss, W. Van't Hof and R. Wagey, *Stem Cells Transl. Med.*, 2013, **2**, 871–883.